The 2009 IEEE/RSJ International Conference on
Intelligent Robots and Systems
October 11-15, 2009 St. Louis, USA

A Hybrid Receding Horizon Control Method for Path Planning in Uncertain Environments

Bin Xu, Andrew Kurdila and Daniel J. Stilwell

***Abstract*—For an autonomous vehicle navigating in a static environment for which an *a priori* map is inaccurate, we propose a hybrid receding horizon control method to determine optimal routes when new obstacles are detected. The hybrid method uses the level sets of the solution to either a global or local Eikonal equation in the formulation of the receding horizon control problem. Whenever an obstacle is detected along the path of the autonomous vehicle, a solution to a local Eikonal equation is used to determine whether a new, global Eikonal equation must be solved for use in the receding horizon optimization problem. The decision to select a new level set solution is made based on certain matching conditions that guarantee the optimality of the path. The selection of a global or local solution to the Eikonal equation induces a hybrid system structure in the control formulation. We rigorously prove sufficient conditions that guarantees that the vehicle will converge to the goal as long as the goal is accessible. In the end, simulation results are discussed.**

I. INTRODUCTION

We consider an autonomous vehicle navigating in a two dimensional static environment for which an *a priori* map is inaccurate. The inconsistency between the *a priori* map and the actual environment may invalidate predefined paths. A fast and effective path replanning method is then required. In this paper, we propose a hybrid receding horizon control strategy that plans minimal risk paths based upon the detection of new obstacles. The proposed method does not account for vehicle dynamics or otherwise addresses issues associated with tracking a particular path. Thus our approach is suited to vehicles that can follow arbitrary paths at potentially slow speeds. This includes certain classes of autonomous surface vehicles, but also includes classes of ground vehicles and ground hovercrafts. We only consider the case that the actual environment has more obstacles compared to the *a priori* map.

The success of the proposed method hinges on the careful and judicious selection of terminal costs in a receding horizon formulation. The terminal cost in this paper is always based on the level sets of a solution to certain Eikonal equations. Recall that if the domain is completely known, it is possible to express the minimum risk path from any point to a target point in terms of the solution to an Eikonal equation [7]. The essence of the approach taken in this paper is that as we encounter new obstacles, previous solutions of Eikonal equations made no provision for the newly discovered obstacles. It is possible to re-calculate a solution to the Eikonal equation over the entire domain whenever a new obstacle is identified, but this can be costly. This paper derives and defines matching conditions between local and old global solutions of related Eikonal equations that guarantee that an optimal path can be found without a new global solution. In order to reduce the computational expense, the proposed method first searches for a minimal risk path locally when the environment changes. If such a path violates these matching conditions, a new solution to the Eikonal equation over the global domain is calculated and used as the terminal cost in a receding horizon formulation.

Our primary contribution in this paper is to formulate a solution to the problem of navigation in a partially known environment in terms of a receding horizon control (RHC) policy such that several challenges in using RHC for autonomous navigation are addressed. Among these challenges, a major one is that the stability of the receding horizon control (see, e.g. [4], [5], [6] and [10]) incorporating a final cost associated with the solutions of Eikonal equations has not yet been well addressed for path planning problems [8]. In addition, the feasible set of states for the vehicle changes as new obstacles are detected. This change of topology often causes the so-called trapping problems such that the vehicle cannot make progress toward the desired endpoint due to the choice of cost functions or a limited planning horizon. Examples of this pathology can be found in papers [12] and [15]. To address the trapping problem, in [1], a cost function generated by a visibility graph that is constructed with respect to the goal is proposed such that the vehicle minimizes the distance to a node in the visibility graph. In [13], a safe bound is added to the vehicle such that the vehicle will not enter any trap smaller than this safe bound. Another challenge is that most current RHC methods for autonomous navigation assume that obstacle geometry is simple and can be modeled as polygons as well as spheres. Closed expressions for obstacle geometry are required in some RHC methods, for example, [1], [13] and [15]. In practice, these assumptions are difficult to justify, particularly for outdoor environments.

This paper addresses the above discussed problems. For the stability issue and trapping problem, we prove, in the framework of [10], that when the map is completely known, the planned trajectory is asymptotically stable in the sense of reaching the goal. For the case that we have an incomplete *a priori* map, we show a sufficient condition that guarantees the vehicle to converge to the goal so long as there exists a feasible path in the updated map. The proposed method is devised in the framework of the fast marching method ([11] and [14]). The fast marching method presumes that the

Bin Xu and Daniel J. Stilwell are with the Bradley Department of Electrical and Computer Engineering, Virginia Polytechnic Institute and State University, Blacksburg, VA, 24061, USA. bxu, stilwell@vt.edu

Andrew J. Kurdila is with the Department of Mechanical Engineering, Virginia Polytechnic Institute and State University, Blacksburg, VA, 24061, USA. kurdila@vt.edu

environment is represented by a two dimensional uniform-sized occupancy grid map. In the presence of obstacles, it marks the corresponding grids to be occupied. Thus, the proposed method does not need to assume that obstacles are polygons.

II. Preliminaries

In this section, we introduce the vehicle model, background for the level sets method as well as the measurement process used to detect new obstacles as they are encountered.

A. Vehicle Model

Consider an autonomous vehicle navigating in $\overline{\Omega} \subset \Re^2$, where Ω is a connected and bounded open set in $\Re^2$. The vehicle will be regarded as a point mass since it is small relative to $\overline{\Omega}$. The task for the vehicle is to travel along an obstacle free path such that the vehicle can reach a predefined goal $\mathbf{z} \in \overline{\Omega}$. Letting the vehicle position at any time t be $\mathbf{x}(t) \in \Re^2$, we model the motion of an autonomous vehicle according to the equation that

$$\dot{\mathbf{x}}(t) = \mathbf{u}(t),\ \mathbf{x}(t_0) = \mathbf{x}_0 \in \overline{\Omega} \tag{1}$$

where $\mathbf{x}(t)$ is the state of the vehicle and $\mathbf{u}(t)$ is the input. We assume that the vehicle moves on a relatively low speed, such that it can turn without forward motion and make a sudden stop. The assumption is reasonable since we are concerned with altering the heading of the vehicle such that it does not move toward obstacles. Then, we can model the admissible input as $\mathbf{u}(t) \in \mathbb{U}$, where

$$\mathbb{U} = \left\{ \mathbf{u} \in \Re^2 :\ \|\mathbf{u}\| \leq v_{\max} \right\} \tag{2}$$

and $v_{\max}$ is a scaler corresponding to the maximum speed of the vehicle.

B. Optimal Trajectories For Known Geometry and The Eikonal Equation

We review some of the well-known characterizations of optimal trajectories when the environment is completely known. For each point $\boldsymbol{\xi}$ in $\overline{\Omega}$, we associate a risk for the vehicle to traverse $\boldsymbol{\xi}$ by a cost function $g \in C^1(\overline{\Omega};\Re)$, which is positive everywhere except at the goal $\mathbf{z}$, for which $g(\mathbf{z}) = 0$. For any $\boldsymbol{\xi} \in \overline{\Omega}$, we define a function $Q(\boldsymbol{\xi})$ to be minimal cumulative cost to travel from $\boldsymbol{\xi}$ to $\mathbf{z}$ as follows

$$Q(\boldsymbol{\xi}) = \min_{\mathbf{c}} \int_0^1 g(\mathbf{c}(p)) \left\| \mathbf{c}'(p) \right\| dp \tag{3}$$

where $\mathbf{c} \in Lip([0,1];\overline{\Omega})$ is a Lipschitz continuous parameterized path with $\mathbf{c}(0) = \boldsymbol{\xi}$ being a current starting point, and $\mathbf{c}(1) = \mathbf{z}$ being the goal (see e.g. [9] pp. 116). It is well-known (see, e.g. [7]) that the solution of this optimization problem is characterized by the solution of the Eikonal equation

$$\|\nabla Q(\boldsymbol{\xi})\| = g(\boldsymbol{\xi}),\ Q(\mathbf{z}) = 0. \tag{4}$$

The optimal paths are along the gradient of level sets. For example, Fig. 1(a) and 1(b) show an example of an *a priori* map, its corresponding contours of level sets and a typical path.

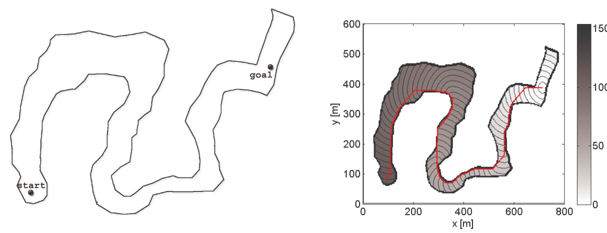

(a) (b)

Fig. 1. (a) An *a priori* map $\overline{\Omega}$. (b) The level sets contours and the optimal path for the *a priori* map.

C. Unmarked Obstacle Detection and New Eikonal Equation

As noted, there are unmarked obstacles due to the inconsistency between the *a priori* map and the actual environment. Denote the actual environment Ω and the initial *a priori* map $\Omega(0)$ that is a bounded open set in $\Re^2$. We assume that $\Omega \subseteq \Omega(0)$. This is consistent with the requirement that actual environment has unexpected obstacles compared to the initial *a priori* map. We denote the set of unmarked obstacle by the closure of an open set O in $\Re^2$ which satisfies $O = \Omega(0) \setminus \overline{\Omega}$.

Let the detection range of an onboard sensor be r, and suppose that measurements are made at a period of h. Letting

$$t_k = t_0 + kh, \forall k = 1,2,3,\ldots, \tag{5}$$

we denote $\Omega(k)$ the updated map at t_k. The new geometry $\Omega(k+1)$ depends on the obstacles that the vehicle detects during the time $[t_k, t_k + h]$ and satisfies

$$\Omega(k+1) = \Omega(k) \setminus \overline{(\cup_{t \in [t_k, t_k+h]} B_r(\mathbf{x}(t)) \cap O)} \tag{6}$$

where $B_r(\mathbf{x}(t))$ is an open ball with radius r and center $\mathbf{x}(t)$. Throughout this paper, we assume that at any time t_k, $\Omega(k)$ is connected and $\mathbf{z} \in \overline{\Omega(k)}$.

As noted in Section II-B, when the observation process picks out obstacles in the path of the vehicle, it is possible to define a new Eikonal equation over a strictly smaller domain. For $\boldsymbol{\xi} \in \overline{\Omega(k)}$, the Eikonal equation for $Q_k(\boldsymbol{\xi})$ becomes

$$\|\nabla Q_k(\boldsymbol{\xi})\| = g(\boldsymbol{\xi})|_{\overline{\Omega(k)}},\ Q_k(\mathbf{z}) = 0. \tag{7}$$

where $\boldsymbol{\xi} \in \overline{\Omega(k)}$, $g \in C^1(\overline{\Omega(0)};\Re)$ and $g(\boldsymbol{\xi})|_{\overline{\Omega(k)}}$ denotes the restriction of g to $\overline{\Omega(k)}$. We notice that in contrast to (4), the solution of the above Eikonal calculates the minimal cost to travel from $\boldsymbol{\xi}$ to $\mathbf{z}$ in the set $\overline{\Omega(k)}$.

III. Asymptotic Stability of RHC: Known Geometry

In this section, we show readers that if the map is accurately known, we can apply the methodology proposed in [10] and [6] to prove the asymptotical stability of the trajectory.

We assume that the *a priori* map is accurate, so that the *a priori* map $\Omega(0)$ is equal to the actual environment Ω. We let the implementation horizon to be h which is identical to the sensor's sampling period although there are no new obstacles to be detected in this case. We choose H as the planning horizon where $H \geq h$. We aim to minimize the risk for traversal during the horizon H as well as the expected minimal risk for traversal from the terminal state $\mathbf{x}(t_k+H)$ toward the goal. The receding horizon formulation is then to find the local optimal control and state pair on $[t_k, t_k+H]$ that solve the minimization problem

$$J_k(\mathbf{x}(\cdot)) = \min_{\mathbf{u}(\cdot)\in\mathbb{U}} \int_{t_k}^{t_k+H} g(\mathbf{x}(\tau))|_{\overline{\Omega}} \|\dot{\mathbf{x}}(\tau)\| d\tau + Q(\mathbf{x}(t_k+H)) \tag{8}$$

subject to

$$\begin{cases} \dot{\mathbf{x}}(t) = \mathbf{u}(t), \\ \mathbf{x}(t_0) = \mathbf{x}_0, \\ \mathbf{x}(t_k) = \mathbf{x}(t_{k-1}+h), \\ \mathbf{x}(t) \in \overline{\Omega(k)}, \end{cases} \tag{9}$$

for $k = 0, 1, 2, \ldots, \infty$, where in this case $\Omega(k) \equiv \Omega$. The overall planned trajectory and control on $[t_0, \infty)$ are spliced together from the locally optimal trajectory in the usual way (see, e.g. [4]).

Proposition 1: Assume that the viscosity solution of $Q \in C^1(\overline{\Omega}; \mathfrak{R})$. Define the value function

$$V(\mathbf{x}(t_k)) = J_k(\mathbf{x}(\cdot)). \tag{10}$$

If $V(\mathbf{x}(t_k))$ is continuously differentiable, the goal $\mathbf{z}$ is asymptotically stable.

Proof of Proposition 1: Following the procedure in [10] and [6], we denote by $\mathbf{u}_f(t)$ the admissible feedback controller that ensures the vehicle to be asymptotically stable with respect to $\mathbf{z}$. Given the level set values Q, let the controller $\mathbf{u}_f$ satisfy

$$\mathbf{u}_f(t) = -\gamma(t) v_{\max} \frac{\nabla Q(\mathbf{x}(t))}{\|\nabla Q(\mathbf{x}(t))\|}, \text{ if } \mathbf{x}(t) \neq \mathbf{z}, \tag{11}$$

for all $t \in [t_0, \infty)$, where $\gamma(t) \in (0, 1]$. Thus, we infer that

$$\dot{Q}(\mathbf{x}(t)) = \nabla Q(\mathbf{x}(t)) \cdot \mathbf{u}_f(t) = -g(\mathbf{x}(t))\|\mathbf{u}_f(t)\|. \tag{12}$$

and $Q(\mathbf{x}(t))$ is a control Lyapunov function. Denote the optimal controller that minimizes J_k by $\mathbf{u}^*(t)$ for $t \in [t_k, t_k+H]$. Since $t_{k+1} = t_k + h$ and since $h \leq H$, we can define the admissible controller $\mathbf{u}^+(t)$ satisfying

$$\mathbf{u}^+(t) = \begin{cases} \mathbf{u}^*(t), \ \forall t \in [t_{k+1}, t_{k+1}+H-h], \\ \mathbf{u}_f(t), \ \forall t \in [t_{k+1}+H-h, t_{k+1}+H]. \end{cases} \tag{13}$$

Given the initial state $\mathbf{x}(t_{k+1})$ at t_{k+1}, we define $\mathscr{J}(\mathbf{x}(t_{k+1}), \mathbf{u}^+(\cdot))$ the cost function that is evaluated by $\mathbf{u}^+(\cdot)$ satisfying

$$\begin{aligned} &\mathscr{J}(\mathbf{x}(t_{k+1}), \mathbf{u}^+(\cdot)) \\ :=& \int_{t_{k+1}}^{t_{k+1}+H} g(\mathbf{x}(\tau))\|\mathbf{u}^+(\tau)\| d\tau + Q(\mathbf{x}(t_{k+1}+H)) \end{aligned} \tag{14}$$

Since $J_{k+1}(\mathbf{x}(\cdot))$ is the minimal cost, we obtain the following inequality

$$\begin{aligned} &J_{k+1}(\mathbf{x}(\cdot)) \leq \mathscr{J}(\mathbf{x}(t_{k+1}), \mathbf{u}^+(\cdot)) \\ =& J_k(\mathbf{x}(\cdot)) - \int_{t_k}^{t_k+h} g(\mathbf{x}(\tau))\|\mathbf{u}^*(\tau)\| d\tau - Q(\mathbf{x}(t_k+H)) \\ &+ \int_{t_k+H}^{t_k+h+H} g(\mathbf{x}(\tau))\|\mathbf{u}_f(\tau)\| d\tau + Q(\mathbf{x}(t_k+H+h)) \end{aligned} \tag{15}$$

Since $\mathbf{u}_f(t)$ satisfies (12), together with the inequality (15), we infer that

$$J_{k+1}(\mathbf{x}(\cdot)) - J_k(\mathbf{x}(\cdot)) \leq -\int_{t_k}^{t_k+h} g(\mathbf{x}(\tau))\|\mathbf{u}^*(\tau)\| d\tau \tag{16}$$

Note that $V(\mathbf{z}) = 0$ and for any $\mathbf{x} \neq \mathbf{z}$, $V(\mathbf{x}) > 0$. According to the assumption, $V(\mathbf{x})$ is continuously differentiable with respect to $\mathbf{x}$. From (10) and (16), the following inequality holds

$$\lim_{h\to 0} \frac{V(\mathbf{x}(t_{k+1})) - V(\mathbf{x}(t_k))}{h} \leq -g(\mathbf{x}(t_k))\|\mathbf{u}^*(t_k)\| < 0 \tag{17}$$

which completes the proof for asymptotical stability according to [6]. ■

Note that in the above proof, the closed form of the optimal controller $\mathbf{u}^*$ is not required. The stability is proved by using the optimality property of the cost function $J_k(\mathbf{x}(\cdot))$.

IV. A Receding Horizon Control Approach with an Incomplete *a priori* Map

In this section, we show the receding horizon control when the *a priori* map is not accurate. Suppose at time $t_k \geq t_0$, we have computed $Q_k(\mathbf{x})$ corresponding to the newly updated map $\overline{\Omega(k)}$. A new receding horizon problem seeks to find the state and control pair on the time interval $[t_k, t_k+H]$ that minimizes the functional

$$J_k(\mathbf{x}(\cdot)) = \min_{\mathbf{u}(\cdot)\in\mathbb{U}} \int_{t_k}^{t_k+H} g(\mathbf{x}(\tau))|_{\overline{\Omega(k)}} \|\dot{\mathbf{x}}(\tau)\| d\tau + Q_k(\mathbf{x}(t_k+H)) \tag{18}$$

subject to (9). Just as in equations (8), the above cost function aims to minimize both the risk of traversal during the horizon H and the expected minimal risk for traversal from the terminal state $\mathbf{x}(t_k+H)$ toward the goal. The following proposition characterizes the trajectory that minimizes the above cost function.

Proposition 2: The optimal trajectory to minimize the cost function (18) satisfies, for $t \in [t_k, t_k+H]$

$$\mathbf{u}(t) = \begin{cases} -v_{\max} \frac{\nabla Q_k(\mathbf{x}(t))}{\|\nabla Q_k(\mathbf{x}(t))\|}, & \text{if } \mathbf{x}(t) \neq \mathbf{z}, \\ \mathbf{0}, & \text{otherwise} \end{cases} \tag{19}$$

Moreover, $J_k(\mathbf{x}(\cdot)) = Q_k(\mathbf{x}(t_k))$.

Proof of Proposition 2: The proof is a direct consequence of the conclusions in [7] and [9]. Substituting (19) into the cost function (18), we conclude that $J_k(\mathbf{x}(\cdot)) = Q(\mathbf{x}(t_k))$. ■

V. Hybrid Receding Horizon Control Method

The RHC method proposed in Section IV requires the computation of Q_k whenever an unexpected obstacle is detected. This process can be computationally expensive. Seeking to minimize the frequency to update Q_k, we propose a variant of the above mentioned RHC in which Q_k will be computed less frequently.

A. Preliminaries

In the hybrid RHC method, instead of updating the level sets as soon as the geometry changes, we sometimes continue to use level sets values of the past as the terminal cost in J_k even though the domain has been observed to change. By doing this, we can reduce the frequency with which we must solve an Eikonal equation on the whole domain. For example, at time instant t_k, we may use the level sets Q_j for the time t_j where $t_j \leq t_k$. In order to indicate which level sets are used at time t_k, we introduce a new index $n(k)$ satisfying $n(k) \leq k$.

Our approach to reduce the computational cost associated with solving Q_k for each step replaces this problem with a smaller, local problem. Recall that $Q_k(\boldsymbol{\xi})$ encodes the cost of traveling from point $\boldsymbol{\xi}$ to the goal $\mathbf{z}$. We define $Q_k^*(\boldsymbol{\xi})$ to be the solution of the Eikonal equation

$$\|\nabla Q_k^*(\boldsymbol{\xi})\| = g(\boldsymbol{\xi})|_{\overline{\Omega(k)}},\ Q_k^*(\mathbf{x}(t_k)) = 0. \tag{20}$$

where $\Omega(k)$ is the updated map at t_k and $\mathbf{x}(t_k)$ is the corresponding vehicle's location. In contrast to $Q_k(\boldsymbol{\xi})$, $Q_k^*(\boldsymbol{\xi})$ encodes the cost to travel from $\boldsymbol{\xi}$ to the current location $\mathbf{x}(t_k)$.

B. Steps for the Hybrid Receding Horizon Control

The procedure for the hybrid RHC is summarized in the following steps:

Initialization: Calculate Q_0. Let $n(1) = 0$.

Step 1: At time t_k, we seek the vehicle state and control on $[t_k, t_k + H]$ which minimizes

$$J_k(\mathbf{x}(\cdot)) = \min_{\mathbf{u}(\cdot)\in\mathbb{U}} \int_{t_k}^{t_k+H} g(\mathbf{x}(\tau))|_{\overline{\Omega(k)}} \|\mathbf{u}(\tau)\| d\tau + Q_{n(k)}(\mathbf{x}(t_k+H)) \tag{21}$$

subject to (9).

Step 2: If there is no obstacle along the path generated by the controller satisfying

$$\mathbf{u}^*(t) = \begin{cases} -v_{\max} \frac{\nabla Q_{n(k)}(\mathbf{x}(t))}{\|\nabla Q_{n(k)}(\mathbf{x}(t))\|}, & \text{if } \mathbf{x}(t) \neq \mathbf{z}, \\ \mathbf{0}, & \text{otherwise} \end{cases} \tag{22}$$

for $t \in [t_k, t_k + H]$, we let $\mathbf{u}(t) = \mathbf{u}^*(t)$ for $t \in [t_k, t_k + h]$. Then, we let $n(k+1) = n(k)$ and go to *Step 1* for the next optimization interval $[t_{k+1}, t_{k+1} + H]$. We will show that (22) is the optimal controller later in Theorem 1.

Step 3: If there are obstacles along the path generated by $\mathbf{u}^*$ in (22), we solve the Eikonal equation (20) over the set of all points accessible from $\mathbf{x}(t_k)$ during the planning horizon $[t_k, t_k + H]$. Since the maximum speed of the vehicle is $v_{\max}$, the domain that is reachable for the vehicle over the planning horizon is $\overline{B_{v_{\max}H}(\mathbf{x}(t_k))}$, where $B_{v_{\max}H}(\mathbf{x}(t_k))$ is an open ball with radius $v_{\max}H$ and center $\mathbf{x}(t_k)$. Therefore, Q_k^* is computed over the local domain $\overline{B_{v_{\max}H}(\mathbf{x}(t_k)) \cap \Omega(k)}$.

Step 4: For each trajectory that satisfies

$$\mathbf{u}^*(t) = \begin{cases} v_{\max} \frac{\nabla Q_k^*(\mathbf{x}((t)))}{\|\nabla Q_k^*(\mathbf{x}((t)))\|}, & \text{if } \mathbf{x}(t) \neq \mathbf{z} \\ \mathbf{0}, & \text{otherwise,} \end{cases} \tag{23}$$

we check if the following two matching conditions hold for $\mathbf{u}^*(t)$,

Condition 1 (Convergence Condition):

$$\frac{1}{v_{\max}} \mathbf{u}^*(t) \cdot \nabla Q_{n(k)}(\mathbf{x}(t)) \leq -\gamma \|\nabla Q_{n(k)}(\mathbf{x}(t))\|,\ \forall \tau \in [t_k, t_k + h] \tag{24}$$

where $\gamma \in (0, 1]$ is a predefined constant.

Condition 2 (Optimality Condition):

$$\nabla Q_k^*(\mathbf{x}(t_k + H)) = -\nabla Q_{n(k)}(\mathbf{x}(t_k + H)). \tag{25}$$

If there exists a $\mathbf{u}^*(t)$ such that both conditions hold, we let $\mathbf{u}(t) = \mathbf{u}^*(t)$ and implement $\mathbf{u}(t)$ for $t \in [t_k, t_k + h]$. We let $n(k+1) = n(k)$ and go to *Step 1*, indicating that we continue to use the old $Q_{n(k)}$ value for the next receding horizon control (21) for $[t_{k+1}, t_{k+1} + H]$.

Step 5: If there is no such trajectory generated by (23) that satisfies both *Condition 1* and *2*, we recompute Q_k corresponding to the entire domain $\overline{\Omega(k)}$ and seek $\mathbf{u}(t)$ such that the cost function (18) is minimized. Then, we set $\mathbf{u}$ to be (19). We let $n(k+1) = k$ and go to *Step 1* which indicates that we use Q_k for the next receding horizon control (21) for $[t_{k+1}, t_{k+1} + H]$.

We stop the process when the vehicle reaches the goal.

We now justify the proposed hybrid receding horizon control algorithm.

Theorem 1: Consider the hybrid receding horizon control algorithm summarized in *Step 1* through *Step 5*. We have the following:

(a) Assume there exists a finite time $t_N \geq t_0$ such that

$$Q_{n(k)}(\boldsymbol{\xi}) = Q_N(\boldsymbol{\xi}),\ \forall \boldsymbol{\xi} \in \Omega(N) \tag{26}$$

for all $t_k \geq t_N$. Assume that $Q_N(\boldsymbol{\xi})$ is continuously differentiable with respect to $\boldsymbol{\xi}$. Then, $\mathbf{x}(t) \to \mathbf{z}$ as $t \to \infty$.

(b) For *Step 2*, if there is no obstacle along the trajectory generated by the control $\mathbf{u}^*$ in (22), $\mathbf{u}^*$ is the control input that minimizes the cost function (21).

(c) For *Step 4*, if *Condition 2* holds, the control input that necessarily minimizes the cost function (21) is (23).

Remark 1: Such finite time t_N required in the assumption of Theorem 1(a) exists in reality. Since an on-board sensor does not appreciate an obstacle that is infinitely small, the newly detected obstacles can be assumed to be bigger than a certain size. Thus, there are finite number of obstacles in the bounded domain $\overline{\Omega(0)}$. Since *Step 2* indicates that the global level sets Q_k does not need to be recomputed unless there is an obstacle on trajectory (22), the global level sets will only be updated finite times. Thus, the time t_N exists and level sets are not updated after t_N.

Proof of Theorem 1: We first show (a). Given the assumption that the global level sets Q_k are not updated after the time t_N, we infer that the vehicle travels along the trajectories generated either by (22) or (23). First, if the vehicle is moving along (22) for some $t_k \geq t_N$, we can derive the following inequality

$$\frac{1}{v_{\max}}\mathbf{u}(t)\cdot\nabla Q_N(\mathbf{x}(t)) = -\|\nabla Q_N(\mathbf{x}(t))\| \leq -\gamma\|\nabla Q_N(\mathbf{x}(t))\|. \tag{27}$$

Second, if vehicle's optimal controller is (23), we can infer that for some time $t_k \geq t_N$, there are some obstacles detected but *Condition 1* is not violated for all $t \in [t_k, t_k+h]$. Both cases indicate that for all $t \geq t_N$ the following inequality holds in either cases

$$\frac{1}{v_{\max}}\mathbf{u}(t)\cdot\nabla Q_N(\mathbf{x}(t)) \leq -\gamma\|\nabla Q_N(\mathbf{x}(t))\|. \tag{28}$$

We take $Q_N(\mathbf{x}(t))$ as a Lyapunov function. Given (28), for all $\mathbf{x}(t) \neq \mathbf{z}$, the following inequality holds

$$\dot{Q}_N(\mathbf{x}(t)) = \mathbf{u}(t)\cdot\nabla Q_N(\mathbf{x}(t)) \leq -v_{\max}\gamma\|\nabla Q_N(\mathbf{x}(t))\| < 0. \tag{29}$$

Thus, we infer that for any initial condition $\mathbf{x}(t_0) \in \overline{\Omega}$, $\mathbf{x}(t) \to \mathbf{z}$ as $t \to \infty$.

We now show (b). From the result of Proposition 2, the cost function (21) satisfies

$$J_k \geq Q_{n(k)}(\mathbf{x}(t_k)). \tag{30}$$

The assumption of (b) indicates that the trajectory generated by (22) is obstacle-free. Thus, substituting (22) into (21), we obtain $J_k(\mathbf{x}(\cdot)) = Q_{n(k)}(\mathbf{x}(t_k))$, which completes the proof.

The last step is to show (c). We first discuss the case when $\mathbf{x}(t) \neq \mathbf{z}$. We adjoin the system differential equation (1) to $J_k(\mathbf{x}(\cdot))$ with multiplier $\boldsymbol{\lambda}(t) \in \Re^2$ (see e.g. [2], pp. 48):

$$\begin{aligned}&\overline{J}_k(\mathbf{x}(\cdot))\\ &= \min_{\mathbf{u}(\cdot)\in\mathbb{U}}\Big(\int_{t_k}^{t_k+H} g(\mathbf{x}(\tau))\|\mathbf{u}(\tau)\| + \boldsymbol{\lambda}^T(\tau)(\mathbf{u}(\tau)-\dot{\mathbf{x}}(\tau))d\tau\\ &\quad + Q_{n(k)}(\mathbf{x}(t_k+H))\Big)\end{aligned} \tag{31}$$

Denoting the Hamiltonian by

$$\mathscr{H}(\mathbf{x}(t),\mathbf{u}(t)) = g(\mathbf{x}(t))\|\mathbf{u}(t)\| + \boldsymbol{\lambda}^T(t)\mathbf{u}(t), \tag{32}$$

we obtain the necessary condition for the optimality that requires the following Euler-Lagrange equations to hold:

$$\boldsymbol{\lambda}(t_k+H) = \frac{\partial Q_{n(k)}^T}{\partial \mathbf{x}}(t_k+H), \tag{33}$$

$$\dot{\boldsymbol{\lambda}}(t) = -\frac{\partial \mathscr{H}^T}{\partial \mathbf{x}}(t) = -\frac{\partial g^T}{\partial \mathbf{x}}(t)\|\mathbf{u}(t)\|, \tag{34}$$

and

$$\frac{\partial \mathscr{H}^T}{\partial \mathbf{u}}(t) = \frac{g(\mathbf{x}(t))\mathbf{u}(t)}{\sqrt{\mathbf{u}^T(t)\mathbf{u}(t)}} + \boldsymbol{\lambda}(t) = \mathbf{0}. \tag{35}$$

Substituting (20) and (23) into (34) yields

$$\begin{aligned}\dot{\boldsymbol{\lambda}}(t) &= -\frac{\partial g^T(\mathbf{x}(t))}{\partial \mathbf{x}}(t)\|\mathbf{u}(t)\| = -\frac{\partial\|\nabla Q_k^*(\mathbf{x}(t))\|}{\partial \mathbf{x}(t)}v_{\max}\\ &= -\frac{\partial^2 Q_k^*}{\partial \mathbf{x}^2}\frac{v_{\max}\nabla Q_k^*(\mathbf{x}(t))}{\|\nabla Q_k^*(\mathbf{x}(t))\|} = -\frac{\partial^2 Q_k^*}{\partial \mathbf{x}^2}\mathbf{u}(t).\end{aligned} \tag{36}$$

Given the boundary condition (33) and given *Condition 2*, integrating the above equation with respect to t yields for $t \in [t_k, t_k+H]$

$$\boldsymbol{\lambda}(t) = -\frac{\partial Q_k^{*T}}{\partial \mathbf{x}}(t). \tag{37}$$

Substituting (37) and (23) into the left side of (35) yields

$$\begin{aligned}&\frac{g(\mathbf{x}(t))\mathbf{u}(t)}{\sqrt{\mathbf{u}^T(t)\mathbf{u}(t)}} + \boldsymbol{\lambda}(t) = \frac{v_{\max}g(\mathbf{x}(t))\nabla Q_k^*(\mathbf{x}(t))}{v_{\max}\|\nabla Q_k^*(\mathbf{x}(t))\|} - \frac{\partial Q_k^{*T}}{\partial \mathbf{x}}(t)\\ &= \frac{\partial Q_k^{*T}}{\partial \mathbf{x}}(t) - \frac{\partial Q_k^{*T}}{\partial \mathbf{x}}(t) = \mathbf{0}.\end{aligned} \tag{38}$$

Therefore, we can conclude that the equality of (35) holds.

If $\mathbf{z}$ is on the trajectory (23), since $\mathbf{u}(t)$ is discontinuous, we treat $\mathbf{z}$ as a corner (see e.g. [2] pp. 125 and [3] pp. 61). Assume that $\mathbf{x}$ reaches $\mathbf{z}$ at time t_k+c, where $c \leq H$. We adjoin the system differential equation (1) to $J_k(\mathbf{x}(\cdot))$ with multiplier $\boldsymbol{\lambda}(t) \in \Re^2$:

$$\begin{aligned}&\overline{J}_k(\mathbf{x}(\cdot))\\ &= \min_{\mathbf{u}(\cdot)\in\mathbb{U}}\int_{t_k}^{t_k+c-0} g(\mathbf{x}(\tau))\|\mathbf{u}(\tau)\| + \boldsymbol{\lambda}^T(\tau)(\mathbf{u}(\tau)-\dot{\mathbf{x}}(\tau))d\tau\end{aligned} \tag{39}$$

Following the standard calculus of variations approach, we infer that the necessary condition for the optimality is

$$\begin{aligned}&\boldsymbol{\lambda}|_{t_k+c-0} = \mathbf{0}, \quad \frac{\partial \mathscr{H}^T}{\partial \mathbf{x}}(t) + \dot{\boldsymbol{\lambda}}(t) = \mathbf{0}\\ &(\mathscr{H} - \boldsymbol{\lambda}^T\dot{\mathbf{x}})|_{t_k+c-0} = 0, \quad \frac{\partial \mathscr{H}^T}{\partial \mathbf{u}}(t) = \mathbf{0}.\end{aligned} \tag{40}$$

Similar to our previous argument for the case when $\mathbf{z}$ is not on the trajectory (23), we can conclude that each equation in (40) holds. Thus, we complete our proof. ■

VI. Simulation

To illustrate the principal conclusions in this paper, we study an example of an autonomous surface vehicle (ASV) navigating in a riverine environment. Fig. 1(a) and 2 respectively represent the *a priori* map and actual environment both of which span an area of $800m \times 600m$. To ensure that an ASV can move freely between empty nodes, the map is discretized with grids size of $3m \times 3m$, which is about twice as large as the specific ASV ($3m \times 1.5m$). The vehicle's detection range is $r = 30m$. We set the fixed parameters that characterize the problem to be $h = 4$ *sec*, $H = 6$ *sec*, $v_{\max} = 3$ m/sec and $\gamma = 0.01$. During the entire mission, there are a total number of fourteen instances where new solutions of the RHC problem were calculated. The location at which each RHC optimization problem is solved is marked by small circles, and they are numbered in order as seen in Fig. 2. Among these calculations, there are thirteen times for which the ASV manages to plan trajectories by computing Q_k^* locally. The only global update occurs at the 14th update when the ASV enters and detects a U-shaped trap shown in the upper right corner of Fig. 2. In the end, Fig. 2 shows that the vehicle eventually reaches the goal.

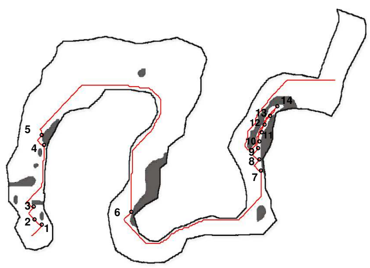

Fig. 2. The gray colored areas are some unexpect obstacles due to the inaccuracy and incompleteness of the *a priori* map in Fig. 1(a). The red line is the actualy course of the ASV.

To illustrate how the update of map information evolves and how the corresponding trajectory changes, we show a sequence of RHC calculations between the 7th to the last instances in Fig. 3(a)-3(c). Between the 7th to the 13th updates shown in Fig. 3(a) and 3(b), since the algorithm finds paths that satisfy both the matching conditions, solutions to the global Eikonal equations do not need to be updated as shown in Fig. 4(a). In Fig. 3(c), since the vehicle detects the dead end, and since the algorithm can not find a path that satisfies one of the matching conditions (*Condition 1*), the level sets Q_k is updated globally. A closeup of the corresponding area is shown in Fig. 4(b). Fig. 3(c) shows that after globally updating Q_k, the vehicle manages to find paths over the next several horizons such that it escapes the dead end eventually.

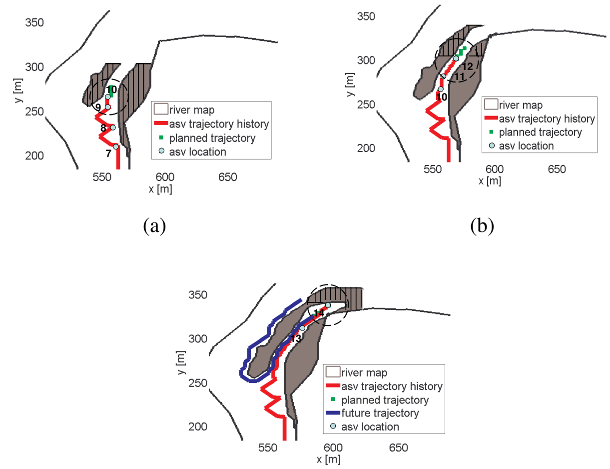

(a) (b) (c)

Fig. 3. (a) The ASV's trajectory history and planned trajectory after the 10th RHC replanning. (b) The ASV's trajectory history and planned trajectory after the 12th RHC replanning. (c) The ASV's trajectory history and planned trajectory in the next few replanning horizons after the 14th RHC replanning. In (a), (b) and (c), the black dash circles represent the planning horizon H and the shaded areas are the new obstacles detected between the planning horizons.

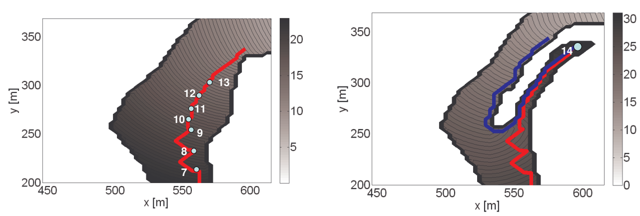

(a) (b)

Fig. 4. (a) The closeup of the global level set that is used as the terminal cost between the 7th to the 13th RHC replannings. (b) The closeup of the level set contour after the global level sets is recalculated at the 14th RHC replanning.

References

[1] J. Bellingham, A. Richards and J.P. How, "Receding Horizon Control of Autonomous Aerial Vehicles," *Proc. of American Control Conference*, 2002.

[2] A.E. Bryson, Jr. and Y.C. Ho, *Applied Optimal Control*, Taylor & Francis, 1975.

[3] I.M. Gelfand and S.V. Fomin, translated and edited by R.A. Silverman, *Calculus of Variations*, Dover Publications, Mineola, NY, 2000.

[4] G.C. Goodwin, M.M. Seron and J.A. De Doná, *Contrstrained Control and Estimation: An Optimisation Approach*, Springer-Verlag, 2005.

[5] A. Jadbabaie, J. Yu and J. Hauser, "Unconstrained Receding Horizon Control of Nonlinear Systems," *Proc. of Conference on Decision and Control*, pp. 3376-3381, 1999.

[6] A. Jadbabaie, J. Yu, and J. Hauser, "Stabilizing receding horizon control of nonlinear systems: a control Lyapunov function approach," *Proc. of the American Control Conference*, pp. 1535–1539, 1999.

[7] R. Kimmel and J.A. Sethian, "Optimal Algorithm for Shape from Shading and Path Planning," *Journal of Mathematical Imaging and Vision*, vol. 14, pp.237-244, 2001.

[8] Y. Kuwata and J.P. How, "Stable Trajectory Design for Highly Constrained Environments using Receding Horizon Control," *Proc. of American Control Conference*, pp. 902-907, 2004.

[9] P.L. Lions, *Generalized Solutions of Hamilton-Jacobi Solutions*, Pitman Publishing INC, 1982.

[10] D.Q. Mayne, J.B. Rawlings, C.V. Rao and P.O.M. Scokaert, "Survey Paper: Constrained model predictive control: Stability and optimality", *Automatica*, no.36, pp. 789-814, 2000.

[11] S.J. Osher and J.A. Sethian, "Fronts propagating with curvature dependent speed: algorithms based on Hamilton-Jacobi formulations," *Journal of Computational Physics*, 79, pp.12-49, 1988.

[12] R. Prazenica, A. Kurdila, R. Sharpley and J. Evers, "Vision-Based Geometry Estimation and Receding Horizon Path Planing for UAVs Operating in Urban Envrionments, " *Proce. of American Control Conference*, 2006.

[13] T. Schouwenaars, J.P. How, and E. Feron, "Receding Horizon Path Planning with Implicit Safety Guarantees," *Proc. of American Control Conference*, 2002.

[14] J.A. Sethian, "Fast Marching Method," *SIAM Review*, vol.41, No.2, pp.199-235, 1999.

[15] M. Zabarankin, A. Kurdila, O. Prokopyev, R. Causey, A. Goel and P. Pardalos, "Optimization Approaches for Vision-Based Path Planning for Autonomous Micro-Air Vechiels in Urban Environments," *Cooperative Networks: Control and Optimization*, Edward Elgar Publishing Ltd, 2008.